



The rheology and gelation of bidisperse 1,4-polybutadiene



D. Roy^a, C.B. Giller^a, T.E. Hogan^b, C.M. Roland^{a,*}

^a Chemistry Division, Code 6126, Naval Research Laboratory, Washington DC 20375-5342, USA

^b Bridgestone Americas, Center for Research and Technology, 1659 S. Main Street, Akron, OH 44301, USA

ARTICLE INFO

Article history:

Received 25 September 2015

Accepted 1 November 2015

Available online 5 November 2015

Keywords:

Polybutadiene

Molecular weight distribution

Gelation

ABSTRACT

1,4-polybutadiene (PB) of varying molecular weight, M , and varying polydispersity (obtained by mixing monodisperse PB) was characterized. As is well-known, some rheological properties are affected by both molecular-weight and polydispersity; however, others show a dependence on M , but not on molecular weight distribution (MWD). We find that the viscosity at constant weight-average M can be accurately accounted for from the ratio of the z - and weight average molecular weights. For M for which the steady-state recoverable compliance, J_s , becomes invariant, no effect of polydispersity on J_s was observed; this observation is contrary to the limited available literature.

Gelation of the PB was also studied. In accord with previous work, the reaction time for network formation and the degree of crosslinking at the gel point both decrease significantly with increasing MWD. The only reliable measure of the gel point for polydisperse samples was from extrapolation of the soluble fraction of networks obtained for various states of cure. Different expressions describing the incipient network of crosslinking polymers were evaluated; these relations were found to be in quantitative mutual accord.

Published by Elsevier Ltd.

1. Introduction

Many properties of polymers are generic, reflecting primarily the large, asymmetric shape of the chain molecules rather than their chemical structure. These properties are often a function of the chain length, so that experimental studies are facilitated by using polymers with monodisperse molecular weights. However, obtaining a narrow molecular weight distribution (MWD) is not always feasible, and so account must be taken of the polydispersity. Moreover, the effect of MWD can depend on the molecular weight, in particular the contribution of chains longer than some “threshold” molecular weight [1–5].

Properties such as the glass transition temperature and fragility [6–8] and for rubbery networks the modulus and strength [9–11] depend inversely on the concentration of chain ends, and thus are determined primarily by the number average molecular weight, M_n . Similarly, the network strands terminating in a free end are elastically ineffective, and thus M_n affects mechanical energy dissipation (hysteresis) [12–14]. For such M_n -dependent properties the effect of MWD is negligible; moreover, at sufficiently high

molecular weight the concentration of chain ends becomes so low that molecular weight effects for such properties generally become negligible [15].

Molecular weight is paramount for the rheological properties of polymers. The viscosity, η , varies nonlinearly with the weight average molecular weight, M_w , but also increases (albeit weakly) with polydispersity at fixed M_w [16,17]. The non-Newtonian flow behavior (e.g., shear-thinning) is influenced by both the molecular weight and its distribution. Elastic properties, such as the recoverable compliance and extrudate swell, generally depend on higher moments of the average molecular weight [18], although the relationships are complex [16]. There have been many investigations of the role of MWD on the rheology of polymers [19–23]. Both theoretical [24–26] and experimental [27–33] works have employed binary blends of monodisperse components in these studies. The dynamics of miscible polymer blends, while more complicated than broad MWD polymers, entail similar issues [34,35]. Analytical and numerical methods have been proposed to extract the MWD from mechanical data [36–41]; these methods are necessarily based on some model. Interpretation of the effect of long-chain branching often requires deconvolution of the effects of MWD, which has led to efforts to understand the latter [42–46].

Since at the gel point the number of crosslinks per chain is independent of chain length [47,48], the naïve expectation is that M_n

* Corresponding author.

E-mail address: roland@nrl.navy.mil (C.M. Roland).

controls gelation. However, the structure of the precursor chains, including their MWD, affects network formation [49–53], and many experiments have been conducted to probe polymers in the vicinity of the gel point, including the distribution of cluster masses [54] and the dynamic mechanical response [55–62].

In this work we examine the influence of MWD on the rheology and network formation in 1,4-polybutadienes (PB) that were either monodisperse or mixtures thereof. Molecular weight is defined by various averages

$$M_i = \frac{\int_0^\infty \hat{n}(M)M^{i+1}dM}{\int_0^\infty \hat{n}(M)M^i dM} \quad (1)$$

where \hat{n} is the number of chains of length M , and $i = 0, 1$, and 2 for the number-, weight-, and z-averages, respectfully. MWD usually refers to the ratio M_w/M_n . This polydispersity parameter is useful for conventional polymers having a range of chain lengths smoothly distributed about the mean, but the details of the distribution may be important. For polymer samples having a low concentration of a high molecular weight component, an alternative measure of MWD is the polydispersity index [63].

$$PDI = \frac{M_{z+1}M_z}{M_w^2} \quad (2)$$

When broadened MWD are achieved by blending, the number- and weight-average molecular weights are given by summation over the averages for the components

$$M_n = \frac{\sum_i w_i}{\sum_i w_i M_{n,i}^{-1}} \quad (3)$$

$$M_w = \frac{\sum_i w_i M_{w,i}}{\sum_i w_i}$$

where w_i is the mass fraction of the i th component. Higher order averages can be calculated from $\hat{n}(M)$ data obtained on the precursor materials by size-exclusion chromatography (SEC).

2. Experimental

Five linear, monodisperse 1,4-polybutadienes (PB; $9.3 \pm 0.2\%$ vinyl content) were synthesized using butyl lithium as the initiator; molecular weights from SEC were in the range from 4.8 to 138 kg/mol. The glass transition of the PB was -98.0 ± 0.2 °C (calorimetric midpoint), except for the lowest molecular weight, for which $T_g = -101.5$ °C. These polymers were blended to give constant M_w or M_n samples with varying degrees of molecular weight polydispersity (Table 1). Representative molecular weight distributions are shown in Fig. 1. Selected monodisperse samples were fractionated and the rheology measured, in order to verify the absence of any high molecular weight “tail” that might not be detected by SEC.

Networks were prepared using 2 phr dicumyl peroxide and curing at 130 °C. Free radical reaction of polybutadiene yields high functionality crosslinks with negligible chain scission [64,65]. The high degree of interspersions of the chains precludes significant intrachain loop formation.

Mixtures were prepared by blending aliquots of the monodisperse PB in methylene chloride. The error in the molecular weights (Table 1) was about 0.5%, governed by the reproducibility of the SEC measurements. Dynamic mechanical measurements employed an Anton-Paar 502, using a 25 mm diameter parallel plates. Steady shearing experiments were carried out using a cone

Table 1
1,4-polybutadiene samples.

Components ^a	M_n^b	M_w^b	M_z^b	M_{z+1}^b	M_w/M_n	PDI
1	129.	138.	149.	165.	1.07	1.29
1	88.4	95.0	102.	112.	1.07	1.27
1	45.6	47.8	50.0	52.4	1.05	1.15
1	24.4	25.8	27.1	28.4	1.06	1.16
1	3.80	4.70	5.41	6.07	1.2	1.49
5	34.9	95.0	126.	138.	2.72	1.93
5	25.9	94.9	130.	142.	3.66	2.05
5	18.6	95.0	137.	148.	5.11	2.25
2	11.1	95.0	152.	158.	8.53	2.66
5	24.5	52.4	80.7	110.	2.14	3.27
5	24.4	89.7	130.	151.	3.68	2.44
2	24.4	121.	147.	158.	4.96	1.60

^a Number of monodisperse polymers comprising the sample.

^b kg/mol.

and plate geometry with either a TA Instruments ARES (25 mm diameter; 0.04 rad cone angle) or an Anton-Paar 702 (50 mm, 0.035 rad).

3. Results

3.1. Rheology

As seen in representative SEC data in Fig. 1, the PB samples prepared by blending monodisperse polymers have multi-modal MWD, rather than a uniform distribution of chain lengths. For this reason polydisperse is the appropriate term, rather than broad MWD. It has been shown for a number of polymers that a plot of the loss tangent versus dynamic modulus (so-called “van Gorp plots” [66]) can be used to distinguish narrow and broad MWD [43,67–69]. The dynamic mechanical data for the PB having the same $M_w = 95$ kg/mol and various polydispersities are plotted in the van Gorp form in Fig. 2. At low frequencies (lower values of G^*) there is a minimum in the loss tangent corresponding to the region of the spectrum with minimal contributions from the terminal and local segmental relaxation modes. The modulus at this minimum is

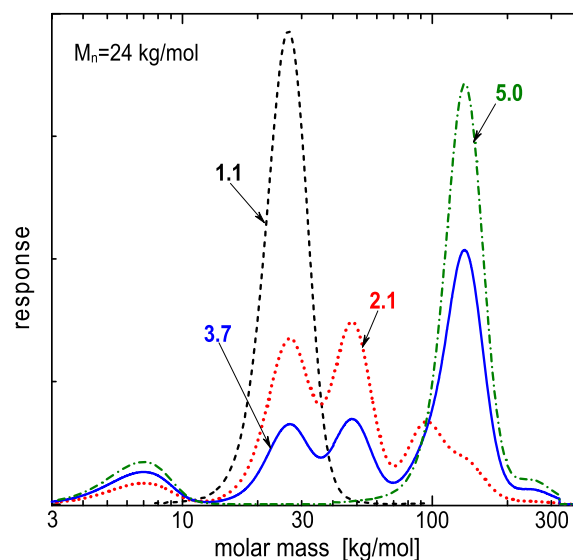


Fig. 1. Molecular weight distributions of four PB having the same M_n , with the polydispersities indicated. The ordinate is the SEC (refractive-index) detector response, the values of which were normalized to equal peak areas. For the more polydisperse samples, the peak molecular weight is much greater than the number average value. Note the abscissa scale is logarithmic.

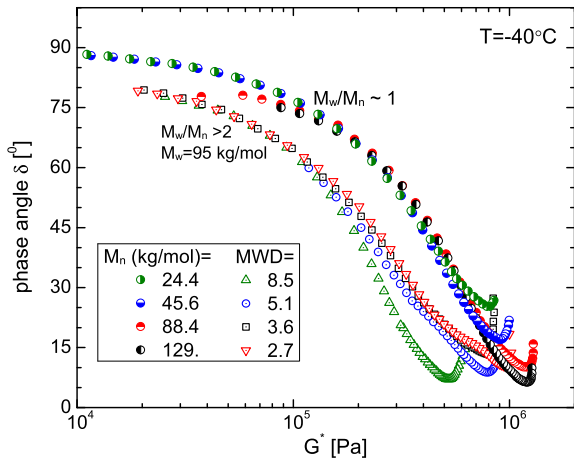


Fig. 2. Arctangent of the loss versus the complex modulus for the PB. At lower values of G^* (lower frequencies) the data group according to whether the polydispersity is near unity or larger. For the latter $M_w = 95$ kg/mol.

close to the plateau modulus [67,70], although the particular value herein is MWD dependent, varying from 0.53 to 1.21. This very broad range encompasses the literature value, $G_N^0 = 1.13 \pm 0.03$ MPa, determined for monodisperse, entangled PB from (truncated) integration of the loss modulus [16].

$$G_N^0 = \frac{2}{\pi} \int_{-\infty}^{\infty} G''(\omega) d \ln \omega \quad (4)$$

from eq. (4), $G_N^0 = 1.12 \pm 0.06$ MPa for the monodisperse PB herein.

Except at lower frequencies, the van Gorp plots for the monodisperse PB coincide, while the data for the polydisperse samples show more divergence. Interestingly, the breadth of the MWD does not affect the latter behavior. These data are thus consistent with the suggestion [67] that van Gorp plots can be used as a qualitative tool to distinguish narrow and broad MWD, even when the latter are bi- or polydisperse. This behavior is due to the smearing out of the terminal zone for broadened molecular weights, so that there is less intensity in the loss modulus, resulting in smaller phase angles on approach to the plateau zone.

The Newtonian viscosities obtained as the limiting values at low frequencies are displayed versus weight average molecular weight in Fig. 3. Included are literature data [71] for PB of similar microstructure. There is good agreement between the data sets, with a fit to all data for $M_w > 6380$ g/mol ($\equiv M_c$, the characteristic value at which the dependence of the viscosity on M_w becomes nonlinear [72]) yielding $\eta_0 \sim M_w^{3.3}$. This exponent is in accord with the literature for strictly monodisperse PB [71]; in fact, it is hard to differentiate in this plot PB having equivalent M_w but different polydispersities. However, as shown in the inset, in which the viscosities for the five samples with $M_w = 95$ kg/mol are plotted on expanded scales, polydispersity increases the viscosity, as must be the case given the nonlinear dependence of η_0 on chain length.

Various equations have been proposed to account for polydispersity. The viscosities of the PB having $M_w = 95$ kg/mol are plotted in Fig. 4 according to an empirical expression [73].

$$\eta_0 \sim M_w^a \left(\frac{M_z}{M_w} \right) \quad (5)$$

The only adjustable parameter, the value of the exponent $a = 3.3$, is obtained from fitting data for the monodisperse samples.

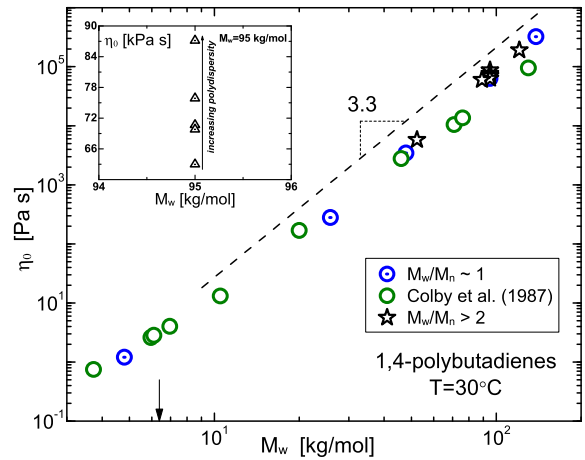


Fig. 3. Zero-shear rate limiting value of the viscosity as a function of weight average molecular weight: monodisperse PB (dotted circles), polydisperse PB (stars), and monodisperse PB adjusted to 30 °C from Ref. [71] (circles). The dashed line is the fit (offset for clarity) yielding $\eta_0 \sim M_w^{3.3}$, and the arrow indicates M_c . The inset shows the data for $M_w = 95$ kg/mol on expanded (linear) scales, indicating the increase in η_0 with increasing polydispersity. Fitting the data for the monodisperse samples only, yields the same dependence, $\eta_0 \sim M_w^{3.3}$.

The viscosities for the polydisperse samples conform well to this equation ($R > 0.99$). Alternative expressions have been proposed to account for polydispersity [73,74].

$$\eta_0 \sim M_w^a \left(\frac{M_w}{M_n} \right)^{0.84} \quad (6)$$

and from the original Doi-Edwards tube model prediction of an M^3 dependence for monodisperse polymers [75].

$$\eta_0 \sim M_w M_z M_{z+1} \quad (7)$$

The latter both describe the present data almost as well ($R > 0.95$) as eq. (5), although eq. (6) has an additional parameter and eq. (7) involves a higher order average of the molecular weight, the measurement of which is more uncertain.

The shear thinning of the viscosity manifested at higher shear rates is an important characteristic of polymeric materials, affecting

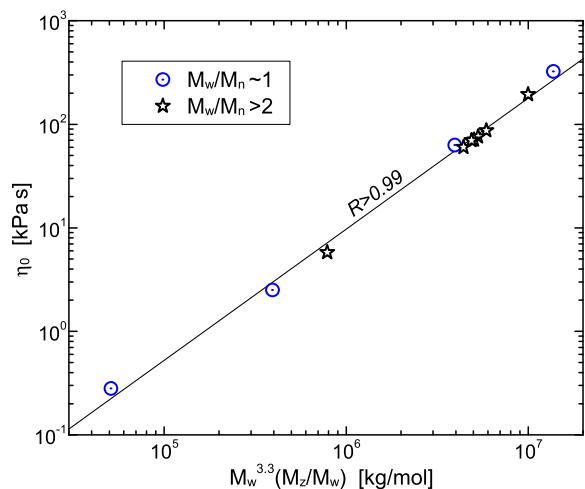


Fig. 4. Zero-shear viscosities of the entangled PB, both monodisperse (dotted circles) and polydisperse (stars) plotted in the form suggested by eq. (5). The correlation coefficient is indicated.

processibility. It is well known that broadening the molecular weight distribution weakens the shear-rate dependence [16,18,76], and one of the motivations for using broad MWD polymers is to make the flow more homogeneous with less melt fracture. Higher moments of the polydispersity than M_w/M_n are reputed to govern the shear thinning behavior [77,78]. There are two distinct aspects of shear thinning: the crossover region at shear rates just beyond the Newtonian regime and the well-developed power-law at higher rates or frequencies.

$$\eta(\dot{\gamma}) \sim \omega^{-m} \quad (8)$$

The shear rate or frequency associated with departure from Newtonian behavior decreases with polydispersity, broadening the crossover regime, and while the available data are limited, the magnitude of the exponent m seems to increase with decreasing MWD [16,18]. Herein we evaluate shear thinning of the dynamic shear viscosity, $\eta^*(\omega)$, because steady flow at shear rates beyond the Newtonian regime resulted in edge fracture. Fig. 5 shows $\eta^*(\omega)$ versus frequency for a mono- and bidisperse PB, each having the same M_w . For the polydisperse sample there is a larger reduction in viscosity with frequency, and the transition to a non-Newtonian frequency-dependence occurs over a broader range of ω . At higher frequencies the broader MWD sample has a lower viscosity than the monodisperse PB, opposite from the behavior in the Newtonian region. The shear thinning of the two PB is very similar in the power-law regime, $d \log \eta^* / d \log \omega \sim \omega^m$ with $m = -0.89 \pm 0.01$. This exponent is very close to literature values for PB of comparable molecular weight [79]. Although the shear thinning slope is essentially invariant to polydispersity, m does depend on molecular weight, as shown in the inset to Fig. 5.

Also included in Fig. 5 are the viscosities calculated using the Gleissle equation [80].

$$\lim_{\dot{\gamma} \rightarrow 0} \eta^+(t, \dot{\gamma}) \Big|_{t^{-1} = \dot{\gamma}} = \eta_{ss}(\dot{\gamma}) \quad (9)$$

where η^+ is the transient viscosity, $\dot{\gamma}$ is the shear rate, and t

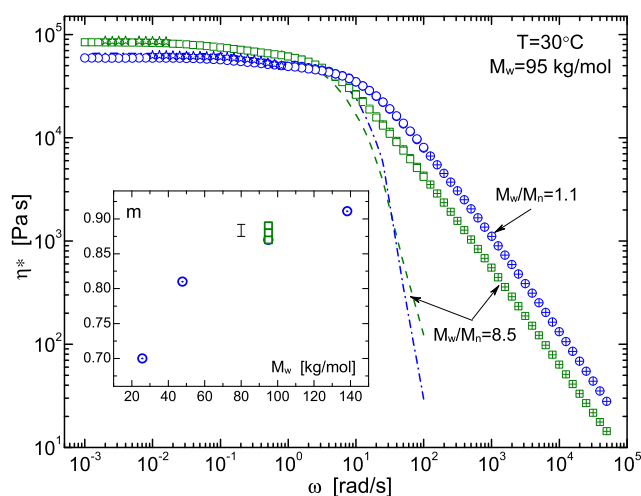


Fig. 5. Dynamic viscosity versus frequency rate for a monodisperse PB (circles) and the most polydisperse sample (squares) having the same weight average molecular weight; symbols with internal crosses are shifted data measured at -40°C . Steady shear data (stars) were limited to the Newtonian regime because of edge fracture; these agree with the dynamic data. The dashed lines represent the viscosities calculated using the Gleissle relation; they are seen to diverge sharply from the measured dynamic viscosities. The inset shows the shear thinning index as a function of molecular weight for monodisperse PB (dotted circles); there is a barely significant increase in m (eq. (8)) with polydispersity at constant molecular weight (squares).

represents the time prior to the onset of steady state flow. In combination with the Cox-Merz rule [81]

$$|\eta^*(\omega)|_{\dot{\gamma}=\omega} = \eta_{ss}(\dot{\gamma}) \quad (10)$$

viscosities in principle can be obtained over a wide range of frequencies or shear rates, using only data obtained at low, Newtonian rates. Although the accuracy of these relations has been found to be good for some materials [82–84], eq. (10) significantly underestimate the $\eta^*(\omega)$ in Fig. 5. Over the limited range of Newtonian behavior, on the other hand, the dynamic and steady viscosities are equivalent for both for both the mono- and bidisperse PB, in accord with eq. (10).

The steady state recoverable compliance, J_s , is a measure of the elastic deformation associated with flow. The most straightforward and reliable measurement of J_s is by creep-recovery experiments, in which configurational reorientations and viscous flow contribute additively. Thus, the ratio of the stress-free recovery following steady-state creep divided by the stress during the creep defines the recoverable compliance. The value at small strain rates, J_s^0 , is the most unambiguous quantity; however, no commercial creep rheometer can measure this linear or “equilibrium” value because their inherent torque induces sample motion that overwhelms the actual recovery. Consequently, J_s^0 data in the literature are quite sparse. With the exception of polystyrene, for which J_s^0 has been measured directly using a custom apparatus having very low internal friction [85], the data in the literature were obtained from the limiting value at low frequency of the storage modulus,

$$J_s^0 = \eta_0^{-2} \lim_{\omega \rightarrow \infty} G'(\omega) \omega^{-2} \quad (11)$$

Given the low magnitude of G' at very low frequencies, application of eq. (11) requires an instrument with negligible compliance and exceptional angular resolution. An alternative method, only applicable to polymers of low enough M_w that flow can be induced without fracture, is from the normal force during steady shearing.

$$J_s^0 = \frac{\Psi_{1,0}}{2\eta_0^2} \quad (12)$$

where $\Psi_{1,0}$ is the first normal stress coefficient (the subscript zero implying the terminal value).

The available literature indicates that J_s^0 becomes constant at sufficiently high molecular weight. This is illustrated in Fig. 6, in which are collected values of J_s^0 for three polymers [86–91]. The abscissa is M_w divided by M_c [72], showing that J_s^0 becomes independent of molecular weight at a high value of $M_w \geq M_c$. (Omitted from Fig. 6 are literature results for the recoverable compliance of PB [29,92,93]. A detailed study using creep-recovery measurements carried out on a magnetic-bearing instrument [94] will be reported in the future.) Although the available data are sparse, it is believed that J_s^0 increases with polydispersity [95,96], even in the high molecular weight regime. If correct, this is an anomaly - a property that does not depend on chain length is affected by the distribution of chain lengths [16].

The recoverable compliance of the PB having $M_w = 95$ kg/mol were determined from steady state shear measurements using eq. (12). This molecular weight is about 15 times M_c [72], so J_s^0 should be independent of molecular weight, at least for the monodisperse polymer. At the low shear rates associated with Newtonian behavior, however, $\Psi_{1,0}$ cannot be measured accurately enough to obtain a reliable determination of J_s^0 . Thus, in Fig. 7 are plotted the recoverable compliance for a range of shear rates beyond the

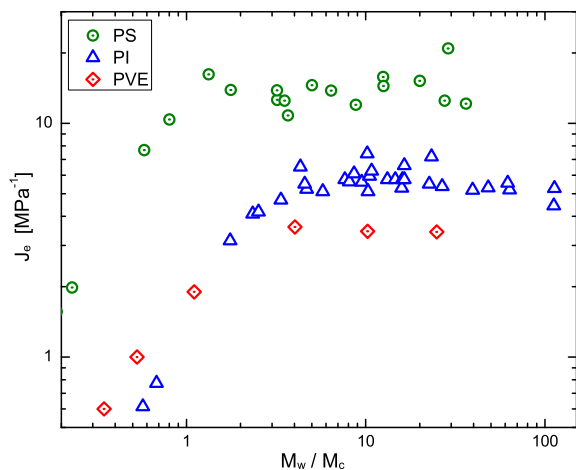


Fig. 6. Steady state recoverable compliance as a function of molecular weight, normalized by the value at which the viscosity dependence on M_w becomes nonlinear: polystyrene (circles) [86,87]; 1,4-polyisoprene (triangles) [88–90]; and polyvinyl-ethylene (diamonds) [91]. Above $M_w/M_c \approx 2-4$, J_e becomes constant.

terminal regime. (Note the increasing uncertainty in the data at lower shear rates; the measurements are limited at high rates by the need to avoid edge fracture.) It can be seen that J_s has no significant dependence on MWD at constant M_w . This is at odds with the suggestion [95,96] that polydispersity causes a marked increase in J_s^0 .

3.2. Gelation

Gelation refers to the liquid-to-solid transition, associated with qualitative differences in properties on either side of the gel point [97]. Upon gelation the polymer becomes insoluble as the shear viscosity becomes asymptotically large [48]. There are semi-quantitative methods to determine the gel-point from viscosity measurements (e.g., ASTM D2471), and in principle the gel point can be deduced by extrapolation to a divergent η . The opposite approach is also possible, estimating the gel-point from the diminution of the equilibrium modulus with reduction in crosslinking.

Empirical gel points have been defined from the extent of

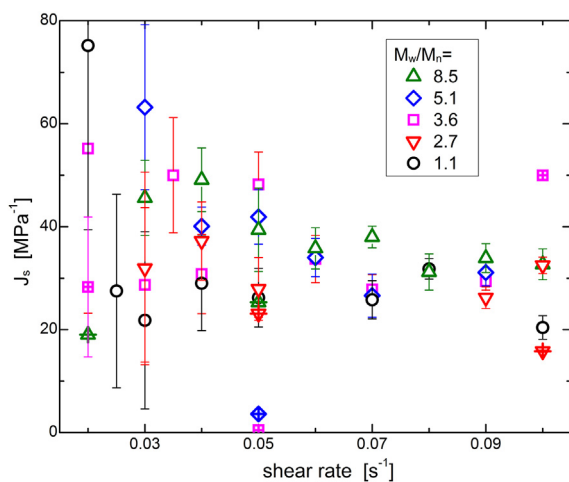


Fig. 7. Steady state recoverable compliance of PB ($M_w = 95$ kg/mol) as a function of shear rate. The rates are higher than the limiting value associated with Newtonian behavior. The open symbols were measured on the TA ARES; the hatched symbols on the Anton-Paar 702. Any effect of MWD on J_s is less than the scatter in the data.

reaction corresponding to equality of the storage, G' , and loss, G'' moduli [55], and from frequency-independence of the loss tangent [55,60,62]. Either of these behaviors is only observed over a limited range of frequencies, and thus can be arbitrary. Near the gel point the dynamic response has the form of a power-law

$$G'(\omega) \propto G''(\omega) \sim \omega^n \quad (13)$$

[55,59], although such behavior is not observed in the absence of formation of large, self-similar hyper-branched structures [98]. The slope ($0 < n < 1$) is affected, *inter alia*, by the network junction functionality [61] and the stoichiometry of the crosslinking reaction [57]. This power-law behavior may extend over a few decades, but at very low frequencies the storage modulus assumes the limiting value for a solid ($G' \sim \text{constant}$) or liquid ($G' \sim \omega^2$).

Herein we determined the gel point using an analysis originally developed by Charlesby and Pinner [99,100] for the radiation crosslinking of polymers. By monitoring the gel fraction as a function of radiation dose, R , the gel point is determined from

$$S + S^{1/2} = A + (2 - A)R_{gel}/R \quad (14)$$

in which R_{gel} is the gel dose and A is a constant. Thus, a plot of the left-hand-side of eq. (14) versus inverse dose extrapolates to R_{gel} at $S + S^{1/2} = 2$. For chemical crosslinking, the cure time, t , is substituted for R

$$S + S^{1/2} = A + (2 - A)\tau_{gel}/t \quad (15)$$

with τ_{gel} representing the time to achieve gelation. (The method of Charlesby and Pinner assumes a constant rate of crosslinking, which is not strictly true for the peroxide reaction herein, which follows first order kinetics.)

Our data for the PB having $M_n = 24$ kg/mol are plotted in the lower panel of Fig. 8, along with the fits of eq. (15). For the monodisperse sample, direct proportionality of $S + S^{1/2}$ and inverse cure time is observed. The obtained gel points for all samples are listed in Table 2. Of course, increasing molecular weight reduces the reaction time required for network formation. MWD also reduces τ_{gel} ; from the monodisperse case ($M_w/M_n \sim 1$) to the most polydisperse system ($M_w/M_n \sim 5$), there is a sixfold reduction in the extent of crosslinking at the gel point.

A second extrapolation method was used based on the number-average crosslinks per chain, z , given by Ref. [101].

$$z = B(S^{-1/(B+1)} - 1)/(1 - S) \quad (16)$$

where $B = M_n/M_w - M_n$. This crosslink density is plotted versus cure time (upper panel of Fig. 8), showing the expected linear relationship. For the monodisperse PB, the time at which z is unity corresponds to the gel point; i.e., $z_{gel} = 1$. As seen in Table 2, these gel points are in excellent agreement with the τ_{gel} determined from eq. (15). For the polydisperse samples, $z < 1$ at the gel point. However, we can use eq. (16) to obtain the value of z_{gel} from the τ_{gel} determined from eq. (15); these results are listed in Table 2. There is a substantial, systematic decrease in the average crosslink density at the gel point with increasing MWD, consistent with the reduction in τ_{gel} with polydispersity.

It has been reported that during crosslinking, a double logarithmic plot of the modulus versus gel fraction will have a slope near unity [102].

$$G' \sim (1 - S)^a \quad (17)$$

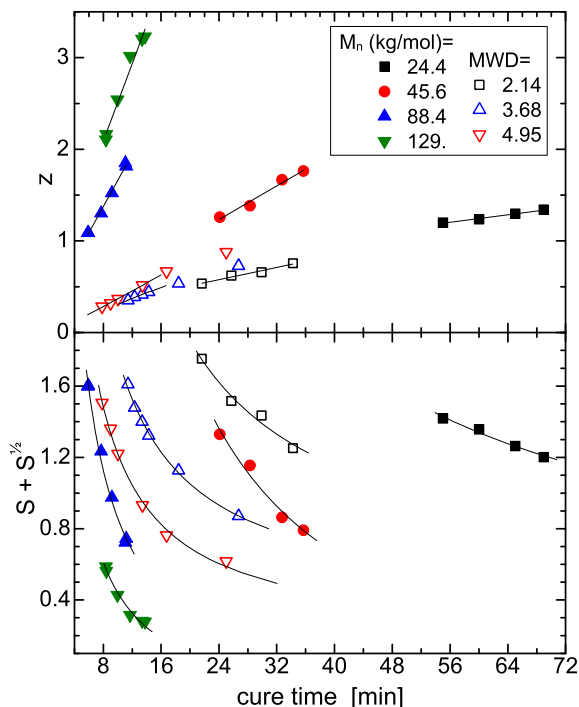


Fig. 8. (Bottom) Soluble fraction data versus cure time; the lines are the fits of eq. (15), with the extrapolation to a value of 2 yielding τ_{gel} . (top) Number of crosslinks per chain (determined from eq. (16)) versus cure time; linear extrapolation to $z = 1$ yields the gel point for monodisperse samples. In both panels, solid symbols denote monodisperse PB, and hollow symbols are $M_n = 24.4$ kg/mol samples with broad MWD. Curing was carried out at 130 °C.

As shown in Table 2, this is approximately true for the polydisperse PB, but not for the monodisperse samples. Thus, eq. (17) is not generally useful for gel point determinations. However, the gel points obtained from eqs. (15) and (16) enable assessment of other methods that rely on the dynamic mechanical properties during curing. In Table 2 are listed the cure times at which $G' = G''$. As can be seen this provides a rough estimate of τ_{gel} , with the error increasing with increasing polydispersity.

Measurements carried out during cure are limited to higher frequencies because the sample is reacting. As an alternative to extend the frequency range, samples were cured for a time equal to the τ_{gel} determined from eq. (15) (Table 2), then quenched to ambient temperature. The dynamic mechanical response was then measured. As seen in Fig. 9, for all samples power-law behavior is limited to about one decade; moreover, the respective slopes for the loss and storage moduli are not equivalent. Generally, the steepness of the curves increases with frequency and decreases with polydispersity.

The data in Table 2 show that the time to reach the gel point decreases with increasing polydispersity. The effect of MWD on

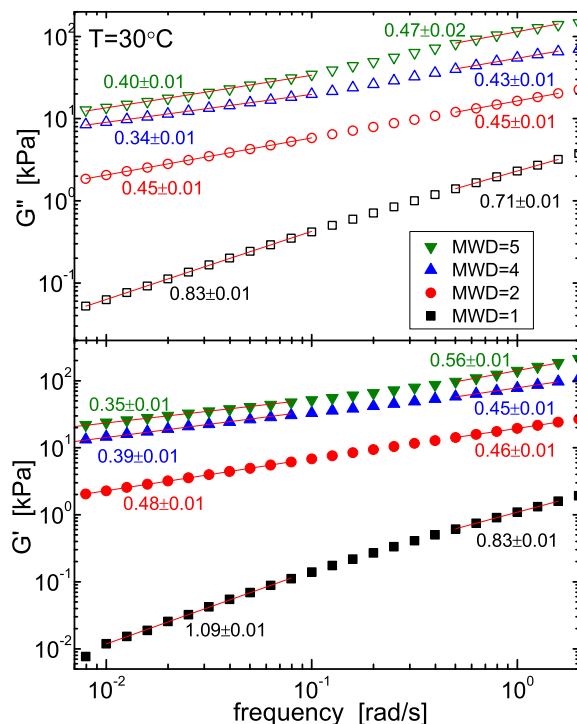


Fig. 9. Dynamic moduli of PB (precursor $M_w = 24$ kg/mol with the indicated polydispersity) reacted to the gel point then quenched. Power-law behavior is limited to narrow spans of frequency; the numbers are the slopes at either end of the measured range.

gelation has been addressed by Miller and Macosko [49], who derived expressions relating the structure to the crosslinking. For systems in which each repeat unit is capable of forming a network junction, the fraction of reacted units at gelation is

$$\alpha_c = [j(M_n/m_0 - 1)]^{-1} \quad (18)$$

where m_0 is the repeat unit molecular ($=54$ g/mol for PB). For a monodisperse molecular weight distribution, $j = 1$, and gelation corresponds to $\alpha_c M_n = 1$, a result originally due to Flory [48]. For a broad MWD, gelation is sometimes taken to correspond to one crosslink per weight average chain [103], but in general this is not correct. When there is a distribution of chain lengths, the value of j (and hence the gel point as discussed above) depends on the distribution. For a Schulz-Zimm MWD, $j = 1.3$; for a most probable distribution, $j = 2$ [49]. For our polydisperse system, we treat j as an adjustable parameter to fit the measured τ_{gel} . To calculate the relative gel times from α_c , we assumed the peroxide is depleted in proportion to $\exp(-t)$. The results for the number of crosslinks per (number average) chain at gelation, z_{gel} , are listed in Table 2. These results are in good agreement with the analysis using eq. (16).

Table 2
Gelation results.

M_n	MWD	Gel point (minutes)		$G' = G''$ (10 rad/s)	a (eq. (17))	z_{gel}	
		$S + S^y = 2$ [eq. (15)]	$z = 1$ [eq. (16)]			eq. (16)	eq. (18)
129,000	1.07	3.1 ± 0.5	3 ± 1	3.4 ± 0.1	3.0 ± 0.3	1.1	1
88,400	1.07	4.9 ± 0.6	5.4 ± 0.5	4.3 ± 0.1	0.86 ± 0.08	0.95	1
45,600	1.05	18 ± 3	19 ± 4	19.8 ± 0.2	2.1 ± 0.4	0.89	1
24,400	1.06	36 ± 6	37 ± 7	48.9 ± 0.1	3.3 ± 0.3	0.95	1
24,500	2.14	18 ± 3	—	17.3 ± 0.1	0.90 ± 0.16	0.51	0.50
24,400	3.65	8.6 ± 0.4	—	5.1 ± 0.3	0.85 ± 0.14	0.27	0.24
24,400	4.95	5.7 ± 0.3	—	3.6 ± 0.4	0.88 ± 0.15	0.16	0.16

4. Conclusions

Studies over many decades have established that for rubbery polymers and to a lesser extent for plastics, the molecular weight and its distribution exert a significant effect on certain properties. In this work chain length distributions were discontinuous, rather than merely broad; our main results for these materials are as follows:

- i. Although M_w is the main parameter governing the zero-shear viscosity, the MWD exerts an effect quantitatively predicted using an empirical relation, eq. (5), that includes M_z [73].
- ii. At higher shear rates the non-Newtonian viscosity shows power-law behavior with a shear-thinning exponent that is essentially independent of MWD. However, the decrease of the viscosity from the Newtonian plateau at low ω is greater for polydisperse samples, and the transition at higher rates to a power-law occurs over a broader frequency range; this smearing out of the transition underlies the improved processability of polymers having broad MWD.
- iii. The steady state compliance measured at rates beyond the terminal zone did not show the reputed anomaly of a MWD-dependence for molecular weights for which J_s^0 is M_w -invariant.
- iv. Mono- and polydisperse samples can be distinguished in dynamic measurements by the different relationship of the phase angle to the complex modulus (van Gurp plots [66]). However, the empirical Gleissle relation significantly underestimates the non-Newtonian viscosities.
- v. It is well known that MWD affects gelation of polymers, with the gel point achieved for lower degrees of crosslinking as MWD increases. The effect of network formation on the dynamic mechanical properties depended on the molecular weight and its distribution, and thus was not useful in determining the onset of gelation. The only method of gel point determination found to be applicable herein was from extrapolation of the soluble fraction of samples cured beyond τ_{gel} . The number of crosslinks per chain necessary for formation of a gel varied from unity for monodisperse PB to a value as low as 0.16 for $M_w/M_n \sim 5$. Different methods used herein to analyze the gelation data gave consistent results.

Acknowledgments

DR and CBG acknowledge postdoctoral fellowships from the Nationals Research Council and the American Society for Engineering Education, respectively. This work was supported by the Office of Naval Research.

References

- [1] B.H. Bersted, T.G. Anderson, *J. Appl. Polym. Sci.* 39 (1990) 499–514.
- [2] J.R. Martin, J.F. Johnson, A.R.J. Cooper, *Macrol. Sci. Rev. Macromol. Chem.* C8 (1972) 57–199.
- [3] D.R. Wiff, M. Gehatia, A.J. Wereta, *J. Polym. Sci. Polym. Phys. Ed.* 13 (1975) 275–284.
- [4] Z. Dobkowski, *Rheol. Acta* 34 (1995) 578–585.
- [5] S.L. Kim, J. Janiszewski, M.D. Skibo, J.A. Manson, R.W. Hertzberg, *Polym. Eng. Sci.* 18 (1979) 145–150.
- [6] R.B. Bogoslovov, T.E. Hogan, C.M. Roland, *Macromolecules* 43 (2010) 2904–2909.
- [7] Y. Ding, V.N. Novikov, A.P. Sokolov, A. Cailliaux, C. Dalle-Ferrier, C. Alba-Simionesco, B. Frick, *Macromolecules* 37 (2004) 9264–9272.
- [8] P.G. Santangelo, C.M. Roland, *Macromolecules* 31 (1998) 4581–4585.
- [9] P.J. Flory, *J. Am. Chem. Soc.* 67 (1945) 2048–2050.
- [10] J. Michel, J.A. Manson, R.W. Hertzberg, *Polymer* 25 (1984) 1657–1666.
- [11] C.M. Kok, *Eur. Polym. J.* 21 (1985) 37–40.
- [12] A.L. Andraday, M.A. Llorente, J.E. Mark, *Polym. Bull.* 28 (1992) 103–108.
- [13] Y.M. Boiko, V.A. Marikhin, V.P. Budtov, B. Turyshev, *J. Polym. Sci. Ser. A* 42 (2000) 1178–1184.
- [14] J.D. Ulmer, W.L. Hergenrother, D.F. Lawson, *Rubber Chem. Technol.* 71 (1998) 637–667.
- [15] R.W. Nunes, J.R. Martin, J.F. Johnson, *Polym. Eng. Sci.* 22 (1982) 205–228.
- [16] W.W. Graessley, *Polymeric Liquids and Networks: Dynamics and Rheology*, Taylor & Francis, New York, 2008.
- [17] F.J. Stadler, C. Piel, J. Kashcta, S. Rulhoff, W. Kaminsky, H. Munstedt, *Rheol. Acta* 45 (2006) 755–764.
- [18] N.G. Kumar, *J. Polym. Sci. Macro. Rev.* 15 (1980) 255–325.
- [19] J. van Meerveld, *J. Non-Newton. Fluid Mech.* 123 (2004) 259–267.
- [20] J.K. Nielsen, H.K. Rasmussen, O. Hassager, G.H. McKinley, *J. Rheol.* 50 (2006) 453–476.
- [21] X. Ye, T. Sridhar, *Macromolecules* 38 (2005) 3442–3449.
- [22] Juliani, L.A. Archer, *J. Rheol.* 45 (2001) 691–708.
- [23] J.G. Oakley, A.J. Giacomin, J.A. Yosick, *Mikrochim. Acta* 130 (1998) 1–28.
- [24] S.J. Park, R.G. Larson, *J. Rheol.* 49 (2005) 523–536.
- [25] F. Léonardi, J.C. Majesté, A. Allal, G. Marin, *J. Rheol.* 44 (2000) 675–692; F. Léonardi, A. Allal, G. Marin, *Rheol. Acta* 46 (2002) 209–224.
- [26] C. Tsenoglou, *Macromolecules* 24 (1991) 1762–1767.
- [27] M. Rubinstein, R.H. Colby, *J. Chem. Phys.* 89 (1988) 5291–5306.
- [28] M. Doi, W.W. Graessley, E. Helfand, D.S. Pearson, *Macromolecules* 20 (1987) 1900–1906.
- [29] M.J. Struglinski, W.W. Graessley, *Macromolecules* 18 (1985) 2630–2643.
- [30] X.P. Yang, A. Halasa, W.L. Hsu, S.Q. Wang, *Macromolecules* 34 (2001) 8532–8540.
- [31] S.F. Wang, S.Q. Wang, A. Halasa, W.L. Hsu, *Macromolecules* 36 (2003) 5355–5371.
- [32] X. Ye, R.G. Larson, C. Pattamaprom, T. Sridhar, *J. Rheol.* 47 (2003) 443–468.
- [33] H. Watanabe, T. Sakamoto, T. Kotaka, *Macromolecules* 18 (1985) 1008–1015.
- [34] J.C. Haley, T.P. Lodge, *J. Rheol.* 48 (2004) 463–486.
- [35] S. Arrese-Igor, A. Alegria, A.J. Moreno, J. Colmenero, *Soft Matter* 8 (2012) 3739–3742.
- [36] S.H. Wasserman, *J. Rheol.* 39 (1995) 601–625.
- [37] W.H. Tuminello, *Polym. Eng. Sci.* 26 (1986) 1339–1347; W.H. Tuminello, W.J. McGrory, *J. Rheol.* 34 (1990) 867–890.
- [38] C. Friedrich, R.J. Loy, R.S. Anderssen, *Rheol. Acta* 48 (2009) 51–162.
- [39] F. Cocchini, M.R. Nobile, *Rheol. Acta* 42 (2003) 232–242; M.R. Nobile, F. Cocchini, *Rheol. Acta* 47 (2008) 509–519.
- [40] T.M. Farias, N.S.M. Cardozo, A.R. Secchi, *J. Braz. Chem. Eng.* 30 (2013) 909–921.
- [41] D.W. Mead, *J. Rheol.* 38 (1994) 1797–1827; D.W. Mead, *J. Rheol.* 40 (1996) 633–661.
- [42] J. Vega, A. Santamaria, A. Munoz-Escalona, P. Lafuente, *Macromolecules* 31 (1998) 3639–3647.
- [43] S.G. Hatzikiriakos, *Polym. Eng. Sci.* 40 (2000) 2279–2287.
- [44] G. Fleury, G. Schlatter, R. Muller, *Rheol. Acta* 44 (2004) 174–187.
- [45] I. Vittorias, M. Parkinson, K. Klimke, B. Debbaut, M. Wilhelm, *Rheol. Acta* 46 (2006) 321–340.
- [46] K. Hyun, M. Wilhelm, *Macromolecules* 42 (2009) 411–422.
- [47] G.S. Grest, K. Kremer, *J. Phys. Fr.* 51 (1990) 2829–2842.
- [48] P.J. Flory, *Principles of Polymer Chemistry*, Cornell University Press, Ithaca, 1953.
- [49] D.R. Miller, C.W. Macosko, *J. Polym. Sci. Polym. Phys. Ed.* 25 (1987) 2441–2469; D.R. Miller, C.W. Macosko, *J. Polym. Sci. Polym. Phys. Ed.* 26 (1988) 1–54.
- [50] M. Demjanenko, K. Dusek, *Macromolecules* 13 (1980) 571–579.
- [51] K. Dusek, M. Duskova-Smrckova, J. Huybrechts, A. Durackova, *Macromolecules* 46 (2013) 2767–2784.
- [52] D.S. Pearson, W.W. Graessley, *Macromolecules* 11 (1978) 528–533.
- [53] M. Lazar, R. Rado, J. Rychly, *Adv. Polym. Sci.* 95 (1990) 149–197.
- [54] J.L. Braun, J.E. Mark, B.E. Eichinger, *Macromolecules* 35 (2002) 5273–5282.
- [55] J.C. Scanlan, M. Hicks, *J. Rheol.* Acta 30 (1991) 412–418.
- [56] C.Y.M. Tung, P.J. Dynes, *J. Appl. Polym. Sci.* 27 (1982) 569–574.
- [57] H.H. Winter, P. Morganelli, F. Chambon, *Macromolecules* 21 (1988) 532–535.
- [58] H.H. Winter, F. Chambon, *J. Rheol.* 30 (1986) 367–382.
- [59] S.K. Venkataraman, L. Coyne, F. Chambon, M. Gottlieb, H.H. Winter, *Polymer* 30 (1989) 2222–2226.
- [60] F. Chambon, H.H. Winter, *J. Rheol.* 31 (1987) 683–697.
- [61] T. Tixier, P. Tordjeman, G. Cohen-Solal, P.H. Mutin, *J. Rheol.* 48 (2004) 39–51.
- [62] S.A. Madbouly, T. Ougizawa, *J. Macromol. Sci. Phys.* B43 (2004) 655–670.
- [63] W.W. Graessley, *J. Polym. Sci. Polym. Phys. Ed.* 18 (1980) 27–34.
- [64] G.G.A. Bohm, J.O. Tveekrem, *Rubber Chem. Technol.* 55 (1982) 575–668.
- [65] M. Akiba, A.S. Hashim, *Prog. Polym. Sci.* 22 (1997) 475–521.
- [66] M. van Gurp, J. Palmen, in: A. Ait-Kadi, J.M. Dealy, D.F. James, M.C. Williams (Eds.), *Proceedings XII International Congress of Rheology*, 1996. Quebec City, CA, pp. 134–135; *Rheol. Bull.* 67 (1998) 5–8.
- [67] S. Trinkle, C. Friedrich, *Rheol. Acta* 40 (2001) 322–328.
- [68] I. Vittorias, D. Lilge, V. Baroso, M. Wilhelm, *Rheol. Acta* 50 (2001), 6911–700.
- [69] Y. Chen, H. Zou, M. Liang, P. Liu, *J. Macromol. Sci. B. Phys.* 52 (2013) 924.
- [70] R.G. Larson, T. Sridhar, L.G. Leal, G.H. McKinley, A.E. Likhtman, T.C.B. McLeish, *J. Rheol.* 47 (2003) 809–818.
- [71] R.H. Colby, L.J. Fetters, W.W. Graessley, *Macromolecules* 20 (1987) 2226–2237.
- [72] C.M. Roland, *Viscoelastic Behavior of Rubbery Materials*, Oxford Uni. Press,

- 2011.
- [73] S.H. Wasserman, W.W. Graessley, *Polym. Eng. Sci.* 36 (1996) 852–861.
- [74] G.R. Zeichner, P.D. Patel, *Proc. 2nd World Conf. Chem. Eng.* 6 (1981) 9 (Montreal, CA).
- [75] W.W. Graessley, *J. Polym. Sci. Polym. Phys. Ed.* 18 (1980) 27–34.
- [76] R.S. Porter, J.F. Johnson, *Trans. Soc. Rheol.* 7 (1963) 241–252.
- [77] J.A. Cote, M. Shida, *J. Appl. Polym. Sci.* 17 (1973) 1639–1650.
- [78] W.W. Graessley, L. Segal, *AIChE J.* 16 (1968) 261–267.
- [79] M. Baumgaertel, M.E. De Rosa, J. Machado, M. Masse, H.H. Winter, *Rheol. Acta* 31 (1992) 75–82.
- [80] W. Gleissle, in: G. Astarita, G. Marucci, L. Nicolais (Eds.), *Rheology*, vol. 2, Plenum, NY, 1980, pp. 457–462.
- [81] W.P. Cox, E.H. Merz, *J. Polym. Sci.* 28 (1958) 619–622.
- [82] H.M. Laun, *J. Rheol.* 30 (1986) 459–501.
- [83] P.M. Wood-Adams, *J. Rheol.* 45 (2001) 203–210.
- [84] C.G. Robertson, C.M. Roland, J.E. Puskas, *J. Rheol.* 46 (2002) 307–320.
- [85] D.J. Plazek, *J. Polym. Sci.* 18 (1985) 2630–2643.
- [86] J.-P. Montfort, G. Marin, P. Monge, *Macromolecules* 17 (1984) 1551–1560.
- [87] D.J. Plazek, V.M. O'Rourke, *J. Polym. Sci. A2* 9 (1971) 209–243.
- [88] N. Nemoto, M. Moriwaki, H. Odani, M. Kurata, *Macromolecules* 4 (1971) 215–219;
N. Nemoto, M. Moriwaki, H. Odani, M. Kurata, *Macromolecules* 5 (1972) 531–553.
- [89] J.T. Gotro, W.W. Graessley, *Macromolecules* 17 (1984) 2767–2775.
- [90] D. Auhl, J. Ramirez, A.E. Likhtman, P. Chambon, C. Fernyhough, *J. Rheol.* 52 (2008) 801–835.
- [91] J. Roovers, P.M. Toporowski, *Rubber Chem. Technol.* 63 (1990) 734–746.
- [92] J.M. Carella, W.W. Graessley, L.J. Fetters, *Macromolecules* 17 (1984) 2775–2786.
- [93] J. Roovers, *Polym. J.* 18 (1986) 153–162.
- [94] D.J. Plazek, *J. Polym. Sci. A2* 6 (1968) 621–638.
- [95] H. Leaderman, R.C. Smith, L.C. Williams, *J. Polym. Sci.* 36 (1959) 233–257.
- [96] W.W. Graessley, T. Masuda, J.E.L. Roovers, N. Hadjichristidis, *Macromolecules* 9 (1976) 127–141.
- [97] D. Stauffer, A. Coniglio, M. Adam, *Adv. Polym. Sci.* 44 (1982) 103–158.
- [98] H. Takahashi, Y. Ishimuro, H. Watanabe, *J. Soc. Rheol. Jpn.* 37 (2009) 159–166.
- [99] A. Charlesby, S.H. Pinner, *Proc. R. Soc. Lond. A249* (1959) 367–386.
- [100] G.G.A. Bohm, J.O. Tveekrem, *Rubber Chem. Technol.* 55 (1982) 575–668.
- [101] M. Gottlieb, C.W. Macosko, T.C. Lepsch, *J. Polym. Sci. Polym. Phys. Ed.* 19 (1981) 1603–1617.
- [102] P. Zhang, F. Zhao, Y. Yuan, X. Shi, S. Zhao, *Polymer* 51 (2010) 257–263.
- [103] A. Charlesby, *Proc. R. Soc. Lond. A 222* (1954) 542–557.